Optimal Double Support Zero Moment Point Trajectories for Bipedal Locomotion

Leonardo Lanari and Seth Hutchinson

Abstract— **In this paper, we address the problem of planning optimal zero moment point (ZMP) trajectories for the double support phase in bipedal gaits that alternate between single and double support. This is achieved by allowing pre- and post-actuation during the single support phases. Thus, we solve two coupled problems: exact tracking of a given desired ZMP trajectory in the pre- and post-phases (single support), and determination of the desired ZMP during the transition phase (double support). Both are solved while minimizing the overall control energy. We also provide a formal method to assess how the choice of desired ZMP trajectory during the single support phases impacts the overall energy expended during the footstep cycle. Although the obtained solution may not be physically feasible in general, it represents a benchmark to which alternative feasible solutions may be compared. Our approach generalizes previous results that consider only constant output in the pre- and post-phases e.g., allowing pre- and post-phase output from a family of polynomial splines. We evaluate the approach via simulations.**

I. Introduction

Bipedal gaits typically consist of alternating phases: a double support phase, in which both feet contact the ground and weight is transferred from back to front foot, and a single support phase in which a stance foot contacts the ground while the swing leg transports the other foot to its next desired location. Such gaits are often specified in terms of a trajectory of the zero moment point (ZMP) [1]–[8], leading to the motion planning problem of constructing a center of mass (CoM) trajectory that corresponds to this ZMP reference trajectory.

In this paper, we address the problem of designing an optimal ZMP reference trajectory for the double support phase, which minimizes the energy over the entire footstep cycle. In most approaches, the ZMP trajectory is constant (or nearly so) during the single support phase, but changes rapidly during the double support phase, moving from the rear foot to the front foot (e.g., [2]). This motivates the problem of designing energy efficient ZMP trajectories during the double support phase.

Our approach is to formulate the problem as an output tracking-transition problem [9], in which the ZMP is considered to be the system output. We consider one footstep cycle, which begins in a single support phase, transitions to a double support phase at time t_i, then transitions back to single support at time t_f. To simplify terminology, in the sequel we refer to these phases as the pre-phase, transition phase, and post-phase, respectively. We assume that the desired ZMP trajectory $x^{\mathrm{d}}_{\mathrm{zmp}}$ is specified for the single support phases, and thus our problem is to design $x^{\mathrm{d}}_{\mathrm{zmp}}(t)$ for $t_i \leq t \leq t_f$, so that the total energy over the footstep cycle is minimized.

Since we consider the ZMP as the output of our bipedal walker, it is natural to represent the system using the cart-table model [10], in which the system state is defined in terms of the center of mass position and velocity, x_{c} and $\dot{x}_{\mathrm{c}}$. In this case, we choose to minimize the the input energy of the cart-table, which is a function of the CoM acceleration. As noted in [11], this choice results in enhanced stability of the actual biped. Equivalently, the problem can be formulated as a stable inversion problem for a linear inverted pendulum (LIP), which is the inverse of the cart-table system. The LIP system behavior can be expressed in terms of its stable and unstable dynamics, x_{s} and x_{u}, at which point we may apply methods that we have previously developed in [12], [13] to derive conditions that ensure bounded system trajectories.

By exploiting the zero dynamics during the pre- and post-phase, we can employ pre-actuation and post-actuation to position the CoM to reduce energy expended during the footstep cycle. This is the key point for our approach. We derive both the input to minimize the total cost and the resulting system trajectory x_{c}.

The main contribution of our paper is to derive the minimum energy desired ZMP trajectory for the transition during the double support phase. In addition, we provide a formal method to assess how the choice of the desired ZMP trajectory during the single support phases impacts the overall energy expended during the footstep cycle. For example it has been noted that restraining the single support phase to be constant does not allow a more natural motion where the ZMP moves forward under the supporting foot [14], [15]. Our approach provides an explanation for this. More generally, we extend the approach of [9] (which considers only the case of constant output in the pre- and post-phases) to more general cases, e.g., choosing pre- and post-phase output from a family of polynomial splines. Although the obtained solution may not be physically feasible in general, it represents a benchmark to which alternative feasible solutions may be compared.

The remainder of the paper is organized as follows. In Sections II and III, we present the system model and provide a formal statement of our problem. In Sections IV and V we derive the input and cost for pre- and post-phase tracking; then, in Section VI we formulate the optimal cost for the

L. Lanari is with the Dipartimento di Ingegneria Informatica, Automatica e Gestionale, Sapienza Università di Roma, Via Ariosto 25, 00185 Rome, Italy. E-mail: lanari@diag.uniroma1.it. S. Hutchinson is Professor of Electrical and Computer Engineering at the University of Illinois. E-mail: seth@illinois.edu. This work is supported by the EU FP7 project COMANOID.

transition phase. In Section VII we solve for the optimal control and corresponding CoM trajectory. Finally, in Section VIII, we analyze our results via a set of simulations.

II. System Model

A common approach to ensure a stable walking for a humanoid is to plan a desired ZMP trajectory $x^{\mathrm{d}}_{\mathrm{zmp}}(t)$ and find the corresponding bounded CoM motion $(x^{\mathrm{d}}_{\mathrm{c}}, \dot{x}^{\mathrm{d}}_{\mathrm{c}})$ that will allow the actual ZMP, x_{zmp}, to track the desired one, $x^{\mathrm{d}}_{\mathrm{zmp}}$. This problem has been formulated as a tracking problem for the so-called cart-table model [10]

$$\begin{pmatrix} \dot{x}_{\mathrm{c}} \\ \ddot{x}_{\mathrm{c}} \end{pmatrix} = \begin{pmatrix} 0 & 1 \\ 0 & 0 \end{pmatrix} \begin{pmatrix} x_{\mathrm{c}} \\ \dot{x}_{\mathrm{c}} \end{pmatrix} + \begin{pmatrix} 0 \\ 1 \end{pmatrix} u_{\mathrm{c}} \tag{1}$$

$$x_{\mathrm{zmp}} = \begin{pmatrix} 1 & 0 \end{pmatrix} \begin{pmatrix} x_{\mathrm{c}} \\ \dot{x}_{\mathrm{c}} \end{pmatrix} - \frac{1}{\omega_0^2} u_{\mathrm{c}} \tag{2}$$

with $(x_{\mathrm{c}}, \dot{x}_{\mathrm{c}})$ being the CoM position and velocity while the control input u_{c} coincides with the CoM acceleration $\ddot{x}_{\mathrm{c}}$. In this setting, the solution of an LQR problem with preview has been given in [1].

An alternative approach considers the inverse system of (1) and (2), i.e. the well-known Linear Inverted Pendulum (LIP), driven by the desired ZMP, $x^{\mathrm{d}}_{\mathrm{zmp}}$. To find the stable CoM trajectories, the problem is reformulated as a stable inversion one [16]. The inverting control law

$$u_{\mathrm{c}} = \omega_o^2 (x_{\mathrm{c}} - x_{\mathrm{zmp}}) \tag{3}$$

transforms the cart-table model into the LIP. For both the cart-table and LIP, the system state is defined in terms of the CoM, $(x_{\mathrm{c}}, \dot{x}_{\mathrm{c}})$. Note that if we set $x_{\mathrm{zmp}} = x^{\mathrm{d}}_{\mathrm{zmp}}$, then (3) is the input that constrains the output of the cart-table to be exactly $x^{\mathrm{d}}_{\mathrm{zmp}}$. The resulting state of the LIP, however, is in general diverging. The LIP can also be represented by the vector $(x_{\mathrm{u}}, x_{\mathrm{s}})^T$ defined as

$$\begin{pmatrix} x_{\mathrm{u}} \\ x_{\mathrm{s}} \end{pmatrix} = \begin{pmatrix} 1 & 1/\omega_o \\ 1 & -1/\omega_o \end{pmatrix} \begin{pmatrix} x_{\mathrm{c}} \\ \dot{x}_{\mathrm{c}} \end{pmatrix} = \Phi^{-1} \begin{pmatrix} x_{\mathrm{c}} \\ \dot{x}_{\mathrm{c}} \end{pmatrix} \tag{4}$$

which represents the unstable and stable components of the LIP dynamics rewritten as

$$\dot{x}_{\mathrm{u}} = \omega_o x_{\mathrm{u}} - \omega_o x_{\mathrm{zmp}} \tag{5}$$

$$\dot{x}_{\mathrm{s}} = -\omega_o x_{\mathrm{s}} + \omega_o x_{\mathrm{zmp}} \tag{6}$$

The LIP eigenvalues represent the zero-dynamics for the cart-table relative degree 0 system. This change of coordinates has been introduced in [7], and used also in [17], where the two motions were respectively defined as divergent and convergent components of motion. Note that the unstable state x_{u} coincides with the definition of the Instantaneous Capture Point of [18] also named as Extrapolated Center of Mass of [19], where the varying terminologies were chosen to highlight salient aspects of the system.

To avoid confusion, we stress that when x_{zmp} is seen as an output we will implicitly refer to the cart-table system, while if we consider x_{zmp} as an input we automatically indicate the LIP system.

III. Problem Statement

In this paper, we consider the problem of constructing the optimal ZMP trajectory and corresponding input for the cart-table system given in (1) and (2) over a footstep cycle of single support, double support, single support. This is illustrated in Figure 1, in which the three stages are labeled as pre-actuation, transition, and post-actuation, respectively. We assume that a trajectory planner has determined the desired ZMP trajectory during pre- and post-phases which are from now on considered as given.

The transition phase occurs during the interval $[t_i, t_f]$, and our problem is to solve for a $x^{\mathrm{d}}_{\mathrm{zmp}}(t)$ in $t_i \leq t \leq t_f$ which minimizes the energy for all t (not only during the transition phase).

Our problem has therefore 2 components: exact tracking of the given desired ZMP in the pre- and post-phases, and determination of the desired ZMP in the transition phase. Both must be solved while minimizing the overall control energy. The approach that we develop below provides an expression for this overall control energy that is parameterized by $x_{\mathrm{s}}(t_f)$ and $x_{\mathrm{u}}(t_i)$.

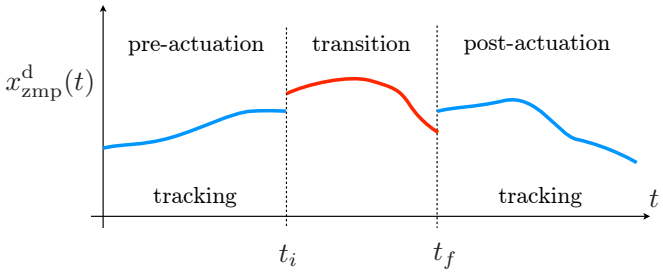

Fig. 1. The three phases of interest: pre-actuation (tracking), transition (double support) and post-actuation (tracking).

In the tracking phases (pre and post) we exploit the concept of zero-dynamics: we can constrain the output of the cart-table system to be exactly $x^{\mathrm{d}}_{\mathrm{zmp}}$ while still having dynamics evolving (the unstable zero-dynamics) forced by $x^{\mathrm{d}}_{\mathrm{zmp}}$, i.e. the LIP dynamics (5)-(6) with input $x^{\mathrm{d}}_{\mathrm{zmp}}$. We first need to select, among all the LIP state evolutions, only the bounded ones; this will be achieved by the use of the boundedness constraint introduced in [12]. Subsequently, only one of these will be chosen as to minimize the overall energy.

For the LIP equations (5)-(6) driven by $x^{\mathrm{d}}_{\mathrm{zmp}}$, the boundedness condition of [12] provides a constraint on x_{u}

$$x^*_{\mathrm{u}}(t; x^{\mathrm{d}}_{\mathrm{zmp}}) = \omega_o \int_0^\infty e^{-\omega_o \tau} x^{\mathrm{d}}_{\mathrm{zmp}}(t+\tau) d\tau \tag{7}$$

By choosing $x_{\mathrm{u}} = x^*_{\mathrm{u}}$, for a given $x^{\mathrm{d}}_{\mathrm{zmp}}$, we ensure that the unstable dynamics remain bounded for any choice of x_{s}. We choose, among all the possible stable x_{s} evolutions,

$$x^*_{\mathrm{s}}(t; x^{\mathrm{d}}_{\mathrm{zmp}}) = \omega_o \int_0^\infty e^{-\omega_o \tau} x^{\mathrm{d}}_{\mathrm{zmp}}(t-\tau) d\tau \tag{8}$$

The $x^{\mathrm{d}}_{\mathrm{zmp}}$ will be obviously chosen in order to guarantee that both integrals exist.

These two $(x_{\rm u}^*, x_{\rm s}^*)$ particular bounded time evolutions, or the corresponding CoM $(x_{\rm c}^*, \dot{x}_{\rm c}^*)$ ones, are asymptotic behaviors which we call *delimiting state evolutions*[1]. These will ensure exact tracking of $x_{\rm zmp}^{\rm d}$, however these are not the only ones. This is schematically shown in Fig. 2 where different bounded CoM trajectories, all guaranteeing exact tracking of the desired $x_{\rm zmp}^{\rm d}$, are reported. These can be parametrized by the value $x_{\rm c}(t_i)$. In the following a constructive analysis is carried out more conveniently in the $(x_{\rm u}, x_{\rm s})$ coordinates.

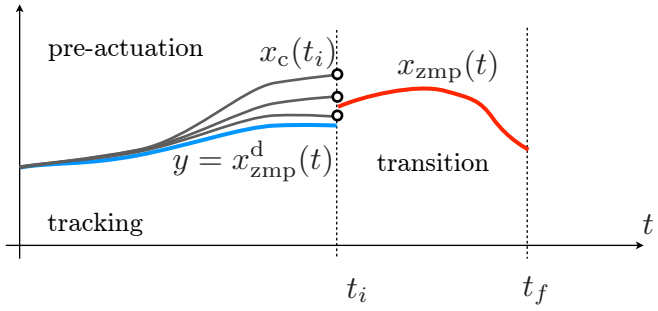

Fig. 2. Pre-actuation: several CoM bounded trajectories guarantee exact tracking of the desired output $x_{\rm zmp}^{\rm d}$.

As is common in the literature [3], [4], [20], [21], we assume that the given desired ZMP trajectory during the pre- and post-phases is defined by a spline of the form

$$x_{\rm zmp}^{\rm d}(t) = \sum_{i=0}^{n} a_i t^i \tag{9}$$

For trajectories given by (9), the choice (8) corresponds to the classic notion of steady state for (6).

Let us define the deviations of the unstable and stable components w.r.t. the delimiting behaviors as

$$e_{\rm u} = x_{\rm u} - x_{\rm u}^*, \qquad e_{\rm s} = x_{\rm s} - x_{\rm s}^* \tag{10}$$

which leads to

$$x_{\rm u} = e_{\rm u} + x_{\rm u}^*, \qquad x_{\rm s} = e_{\rm s} + x_{\rm s}^* \tag{11}$$

and

$$x_{\rm c} = \frac{1}{2}(x_{\rm u} + x_{\rm s}) = \frac{1}{2}(e_{\rm u} + e_{\rm s}) + x_{\rm c}^* \tag{12}$$

Computing the time derivatives, we obtain

$$\begin{aligned} \dot{e}_{\rm u} &= \dot{x}_{\rm u} - \dot{x}_{\rm u}^* \\ &= \omega_o(x_{\rm u} - x_{\rm zmp}^{\rm d}) - \omega_o(x_{\rm u}^* - x_{\rm zmp}^{\rm d}) \\ &= \omega_o e_{\rm u} \end{aligned} \tag{13}$$

since $x_{\rm u}^*$ is also a solution of the unstable dynamics (5). Similarly, for $\dot{e}_{\rm s}$ we obtain

$$\dot{e}_{\rm s} = -\omega_o e_{\rm s} \tag{14}$$

Hence the LIP driven by $x_{\rm zmp}^{\rm d}$ can be rewritten as an autonomous system (13)-(14) in the $(e_{\rm u}, e_{\rm s})$ coordinates.

[1]These can be thought as the steady state evolution for a stable system.

IV. Pre-phase Tracking

In the pre-phase we have a final condition in $t = t_i$, so considering $e_{\rm u}(t)$ as an initial condition we can rewrite the unstable dynamics

$$e_{\rm u}(t_i) = e^{\omega_o(t_i - t)} e_{\rm u}(t), \quad \text{for} \quad t \le t_i \tag{15}$$

as

$$e_{\rm u}(t) = e^{-\omega_o(t_i - t)} e_{\rm u}(t_i), \quad \text{for} \quad t \le t_i \tag{16}$$

Similarly for the stable dynamics

$$e_{\rm s}(t) = e^{\omega_o(t_i - t)} e_{\rm s}(t_i), \quad \text{for} \quad t \le t_i \tag{17}$$

Since we want $x_{\rm u}$ and $x_{\rm s}$ to tend to their delimiting behaviors $x_{\rm u}^*$ and $x_{\rm s}^*$, or equivalently $(e_{\rm u}, e_{\rm s}) \to (0, 0)$, as $t \to -\infty$, we need necessarily

$$e_{\rm s}(t_i) = 0 \quad \text{that is} \quad x_{\rm s}(t_i) = x_{\rm s}^*(t_i) \tag{18}$$

while $e_{\rm u}(t_i)$, and thus $x_{\rm u}(t_i)$ is totally free. Therefore during the pre-phase we have

$$e_{\rm u}(t) = e^{-\omega_o(t_i - t)} e_{\rm u}(t_i), \quad \text{for} \quad t \le t_i \tag{19}$$

$$e_{\rm s}(t) = 0 \tag{20}$$

and the corresponding CoM trajectory for $t \le t_i$ is

$$x_{\rm c}(t) = \frac{1}{2}(e_{\rm u} + e_{\rm s}) + x_{\rm c}^* \tag{21}$$

$$= \frac{1}{2} e^{-\omega_o(t_i - t)} \left(x_{\rm u}(t_i) - x_{\rm u}^*(t_i)\right) + x_{\rm c}^*(t) \tag{22}$$

Therefore we have that for the pre-phase $x_{\rm u}(t_i)$ is still to be determined and (22) defines a family of bounded trajectories which all guarantee exact tracking of $x_{\rm zmp}^{\rm d}$.

The inverting control (3)

$$u^{\rm d} = \omega_o^2(x_{\rm c} - x_{\rm zmp}^{\rm d}) \tag{23}$$

gives the pre-phase explicit parametrized input since we have the explicit expression (22) for $x_{\rm c}(t)$. Note, from (12), that

$$u^{\rm d} = u^{\rm pre} = \frac{\omega_o^2}{2}(e_{\rm s} + e_{\rm u}) + \omega_o^2(x_{\rm c}^* - x_{\rm zmp}^{\rm d}) \tag{24}$$

In the linear case for $x_{\rm zmp}^{\rm d}$, i.e., $n \le 1$ in (9), we can show, based on the specific choice of $x_{\rm s}^*$ in (8), that $x_{\rm c}^* = x_{\rm zmp}^{\rm d}$, and therefore we have the full explicit expression

$$u^{\rm pre}(t) = \frac{\omega_o^2}{2} e_{\rm u}(t) = \frac{\omega_o^2}{2} e^{-\omega_o(t_i - t)} (x_{\rm u}(t_i) - x_{\rm u}^*(t_i)) \tag{25}$$

We can now derive the cost during the pre-actuation stage. Assuming a cost quadratic in the input effort, leads to

$$J_{\rm pre}(x_{\rm u}(t_i)) = \int_{-\infty}^{t_i} \left[u^{\rm pre}(t)\right]^2 dt = \frac{\omega_0^3}{8} \left[e_{\rm u}(t_i)\right]^2 \tag{26}$$

which we generically write as

$$J_{\rm pre}(x_{\rm u}(t_i)) = W_{\rm pre} \ \left[e_{\rm u}(t_i)\right]^2 \tag{27}$$

V. Post-phase Tracking

The derivations for the post-phase tracking are structurally similar to those for the pre-phase tracking, with the exception that here we have initial conditions at $t = t_f$

$$e_{\mathrm{u}}(t) = e^{\omega_o(t-t_f)} e_{\mathrm{u}}(t_f), \quad \text{for} \quad t \geq t_f \tag{28}$$

$$e_{\mathrm{s}}(t) = e^{-\omega_o(t-t_f)} e_{\mathrm{s}}(t_f), \quad \text{for} \quad t \geq t_f \tag{29}$$

Here, x_{u} and x_{s} should tend to their delimiting behaviors x_{u}^* and x_{s}^* as $t \to \infty$, or equivalently $(e_{\mathrm{u}}, e_{\mathrm{s}}) \to (0, 0)$. This leads to

$$e_{\mathrm{u}}(t_f) = 0 \quad \text{that is} \quad x_{\mathrm{u}}(t_f) = x_{\mathrm{u}}^*(t_f) \tag{30}$$

which implies $e_{\mathrm{u}}(t) = 0$, while $e_{\mathrm{s}}(t_f)$, and thus $x_{\mathrm{s}}(t_f)$, is totally free. The corresponding parametrized CoM trajectories are

$$x_{\mathrm{c}}(t) = \frac{1}{2}(e_{\mathrm{u}} + e_{\mathrm{s}}) + x_{\mathrm{c}}^* \tag{31}$$

$$= \frac{1}{2} e^{-\omega_o(t-t_f)} \left(x_{\mathrm{s}}(t_f) - x_{\mathrm{s}}^*(t_f)\right) + x_{\mathrm{c}}^*(t) \tag{32}$$

As for the pre-phase tracking, the input during these tracking phases is given by

$$u^{\mathrm{d}} = \omega_o^2 (x_{\mathrm{c}} - x_{\mathrm{zmp}}^{\mathrm{d}}) \tag{33}$$

$$= \frac{\omega_o^2}{2}(e_{\mathrm{s}} + e_{\mathrm{u}}) + \omega_o^2 (x_{\mathrm{c}}^* - x_{\mathrm{zmp}}^{\mathrm{d}}) \tag{34}$$

with the full explicit expression

$$u^{\mathrm{post}}(t) = \frac{\omega_o^2}{2} e_{\mathrm{s}}(t) = \frac{\omega_o^2}{2} e^{-\omega_o(t-t_f)} (x_{\mathrm{s}}(t_f) - x_{\mathrm{s}}^*(t_f)) \tag{35}$$

Finally, we can define the cost

$$J_{\mathrm{post}}(x_{\mathrm{s}}(t_f)) = \int_{t_f}^{-\infty} \left[u^{\mathrm{post}}(t)\right]^2 dt = \frac{\omega_0^3}{8} \left[e_{\mathrm{s}}(t_f)\right]^2 \tag{36}$$

$$= W_{\mathrm{post}} \ \left[e_{\mathrm{s}}(t_f)\right]^2 \tag{37}$$

VI. Transition Phase

Using the coordinate transformation (4), we can relate the boundary conditions for x_{u} and x_{s} to those for the CoM as

$$x(t_i) = \begin{pmatrix} x_{\mathrm{c}}(t_i) \\ \dot{x}_{\mathrm{c}}(t_i) \end{pmatrix} = \Phi \begin{pmatrix} x_{\mathrm{u}}(t_i) \\ x_{\mathrm{s}}(t_i) \end{pmatrix} = \Phi \begin{pmatrix} x_{\mathrm{u}}(t_i) \\ x_{\mathrm{s}}^*(t_i) \end{pmatrix} \tag{38}$$

$$x(t_f) = \begin{pmatrix} x_{\mathrm{c}}(t_f) \\ \dot{x}_{\mathrm{c}}(t_f) \end{pmatrix} = \Phi \begin{pmatrix} x_{\mathrm{u}}(t_f) \\ x_{\mathrm{s}}(t_f) \end{pmatrix} = \Phi \begin{pmatrix} x_{\mathrm{u}}^*(t_f) \\ x_{\mathrm{s}}(t_f) \end{pmatrix} \tag{39}$$

For the controllable cart-table system (1) with system and input matrices (A, B), the quadratic cost

$$J_{\mathrm{tr}} = \int_{t_i}^{t_f} u^T u \, d\tau \tag{40}$$

is minimized by the optimal input

$$u^{\mathrm{tr}}(t) = B^T e^{A^T(t_f - t)} G_{[t_i,t_f]}^{-1} \mathrm{d}(t_i, t_f) \tag{41}$$

where

$$\mathrm{d}(t_i, t_f) = x(t_f) - e^{A(t_f - t_i)} x(t_i) \tag{42}$$

and $G_{[t_i,t_f]}$ is the controllability grammian, given by

$$G_{[t_i,t_f]} = \int_{t_i}^{t_f} e^{A(t_f-\tau)} B B^T e^{A^T(t_f-\tau)} d\tau \tag{43}$$

$$= \begin{pmatrix} \frac{1}{3}\Delta T^3 & \frac{1}{2}\Delta T^2 \\ \frac{1}{2}\Delta T^2 & \Delta T \end{pmatrix} \tag{44}$$

where $\Delta T = t_f - t_i$.

The optimal cost is then given by

$$J_{\mathrm{tr}}^{\mathrm{opt}} = \mathrm{d}(t_i, t_f)^T G_{[t_i,t_f]}^{-1} \mathrm{d}(t_i, t_f) \tag{45}$$

and depends on the yet unspecified values for $x_{\mathrm{u}}(t_i)$ and $x_{\mathrm{s}}(t_f)$ which we combine in a vector Ψ

$$\Psi = \begin{pmatrix} x_{\mathrm{u}}(t_i) \\ x_{\mathrm{s}}(t_f) \end{pmatrix} \tag{46}$$

From (4) define the two columns of $\Phi = (\Phi_u \Phi_s)$ and M as

$$\Phi_u = \begin{pmatrix} 1/2 \\ \omega_o/2 \end{pmatrix}, \quad \Phi_s = \begin{pmatrix} 1/2 \\ -\omega_o/2 \end{pmatrix}, \tag{47}$$

$$M = e^{A\Delta T} = \begin{pmatrix} 1 & \Delta T \\ 0 & 1 \end{pmatrix} \tag{48}$$

Substituting into (42), straightforward computations lead to

$$d(t_i, t_f) = x(t_f) - e^{A(t_f - t_i)} x(t_i) \tag{49}$$

$$= \begin{pmatrix} -M\Phi_u & \Phi_s \end{pmatrix} \Psi + \begin{pmatrix} -M\Phi_s & \Phi_u \end{pmatrix} \mathbf{f} \tag{50}$$

$$= H_2 \Psi + H_1 \mathbf{f} \tag{51}$$

where $\mathbf{f}$ contains the known quantities

$$\mathbf{f} = \begin{pmatrix} x_{\mathrm{s}}^*(t_i) \\ x_{\mathrm{u}}^*(t_f) \end{pmatrix} \tag{52}$$

The optimal energy cost during the transition phase can then be expressed as a quadratic function of the unknown Ψ

$$J_{\mathrm{tr}}^{\mathrm{opt}} = d(t_i, t_f)^T G_{[t_i,t_f]}^{-1} d(t_i, t_f) \tag{53}$$

$$= \Psi^T H_2^T G_{[t_i,t_f]}^{-1} H_2 \Psi + 2\Psi^T H_2^T G_{[t_i,t_f]}^{-1} H_1 \mathbf{f} + \mathbf{f}^T H_1^T G_{[t_i,t_f]}^{-1} H_1 \mathbf{f} \tag{54}$$

VII. Minimizing the Total Trajectory Cost

In sections IV to VI we have derived the single energy costs in terms of the unknown vector Ψ. The overall total cost J_{tot} can be written as

$$J_{\mathrm{tot}} = J_{\mathrm{pre}} + J_{\mathrm{post}} + J_{\mathrm{tr}}^{\mathrm{opt}} = \Psi^T \Lambda \Psi - 2\Psi^T \mathbf{h} + p \tag{55}$$

with

$$\Lambda = W + H_2^T G_{[t_i,t_f]}^{-1} H_2 \tag{56}$$

$$\mathbf{h} = \left(W - H_2^T G_{[t_i,t_f]}^{-1} H_1\right) \mathbf{f} \tag{57}$$

$$p = \mathbf{f}^T \left(W + H_1^T G_{[t_i,t_f]}^{-1} H_1\right) \mathbf{f} \tag{58}$$

and

$$W = \begin{pmatrix} W_{\mathrm{pre}} & 0 \\ 0 & W_{\mathrm{post}} \end{pmatrix} \tag{59}$$

Therefore, being Λ invertible for the cart-table system, the optimal value of Ψ which minimizes the energy on the whole time domain

$$J_{\rm tot} = \int_{-\infty}^{t_i} \left[u^{\rm pre}(t)\right]^2 dt + \int_{t_i}^{t_f} \left[u^{\rm tr}(t)\right]^2 dt + \int_{t_f}^{\infty} \left[u^{\rm post}(t)\right]^2 dt \tag{60}$$

is given by

$$\Psi^* = \Lambda^{-1}\mathbf{f} \tag{61}$$

while the optimal feedforward input $u^{\rm opt}$ is made of the three inputs, one in each time interval, $u^{\rm pre}$, $u^{\rm tr}$ and $u^{\rm post}$ with the optimal Ψ^*.

VIII. Discussion and Simulations

In order to illustrate the general result readily obtained, we choose the pre- and post- ZMP references to be linear

$$x^{\rm pre}_{\rm zmp}(t) = \alpha^i_1(t - t_i) + \alpha^i_0, \quad x^{\rm post}_{\rm zmp}(t) = \alpha^f_1(t - t_f) + \alpha^f_0 \tag{62}$$

as shown in Fig. 3, i.e. of the form $x^{\rm d}_{\rm zmp}(t) = a \cdot t + b$.

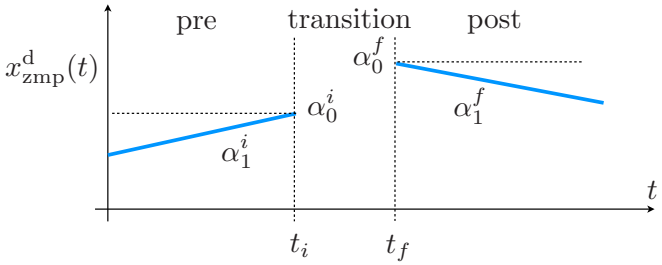

Fig. 3. Generic linear desired ZMP for the single support

For this choice, using (7) and (8) we have

$$x^*_{\rm u}(t) = a\left(t + \frac{1}{\omega_o}\right) + b, \quad x^*_{\rm s}(t) = a\left(t - \frac{1}{\omega_o}\right) + b \tag{63}$$

or equivalently

$$x^*_{\rm c}(t) = \frac{1}{2}(x^*_{\rm u} + x^*_{\rm s}) = a \cdot t + b \tag{64}$$

In the remainder of this section, we develop specific results for three cases: point feet with $\Delta T = 0$, constant $x^{\rm pre}_{\rm zmp}$ and $x^{\rm post}_{\rm zmp}$, and linear $x^{\rm pre}_{\rm zmp}$ and $x^{\rm post}_{\rm zmp}$.

A. Limiting case for point feet

The point-foot case (see [18]), where the position of the foot changes instantaneously between constant values, can be seen as the limiting behavior $\Delta T \to 0$ with $\alpha^i_1 = \alpha^f_1 = 0$. In this case, there would be no transition phase and the continuity of the CoM state at the transition time implies

$$\begin{pmatrix} x_{\rm u}(t_i) \\ x^*_{\rm s}(t_i) \end{pmatrix} \to \begin{pmatrix} x^*_{\rm u}(t_f) \\ x_{\rm s}(t_f) \end{pmatrix} \tag{65}$$

and therefore

$$x_{\rm u}(t_i) = x^*_{\rm u}(t_f) \qquad x^*_{\rm s}(t_i) = x_{\rm s}(t_f) \tag{66}$$

leading to

$$e_{\rm u}(t_i) = x_{\rm u}(t_i) - x^*_{\rm u}(t_i) = x^*_{\rm u}(t_f) - x^*_{\rm u}(t_i) \tag{67}$$

$$e_{\rm s}(t_f) = x_{\rm s}(t_f) - x^*_{\rm s}(t_f) = x^*_{\rm s}(t_i) - x^*_{\rm s}(t_f) \tag{68}$$

Therefore when $\Delta T = 0$ we have the total cost (being $W_{\rm pre} = W_{\rm post}$)

$$J_{\rm pre} + J_{\rm post} = W_{\rm pre}\left(\left[e_{\rm u}(t_i)\right]^2 + \left[e_{\rm s}(t_f)\right]^2\right) \tag{69}$$

which, being for the constant single support phase $x^*_{\rm u}(t_i) = x^*_{\rm s}(t_i)$ and $x^*_{\rm u}(t_f) = x^*_{\rm s}(t_f)$, can also be written as

$$J_{\rm pre} + J_{\rm post} = \Psi^T\Lambda\Psi - 2\Psi^T W\mathbf{f} + \mathbf{f}^T W\mathbf{f} \tag{70}$$

$$= 2W_{\rm pre}(x^*_{\rm u}(t_f) - x^*_{\rm u}(t_i))^2 \tag{71}$$

$$= 2W_{\rm pre}(x^*_{\rm s}(t_f) - x^*_{\rm s}(t_i))^2 \tag{72}$$

In this point foot case, when a unit step length ($\alpha^f_0 - \alpha^i_0 = 1$) is taken at T from $\alpha^i_0 = 0$, being $x^*_{\rm c}(t) = 0$ in the pre-phase and 1 in the post-, from (22) and (32) we recover the following well-known analytical expression of the bounded CoM plotted in Fig. 4.

$$x_{\rm c}(t) = \begin{cases} \frac{1}{2}e^{\omega_o(t-T)}, & \text{if } t \le T \\ \frac{1}{2}(2 - e^{-\omega_o(t-T)}), & \text{if } t \ge T \end{cases} \tag{73}$$

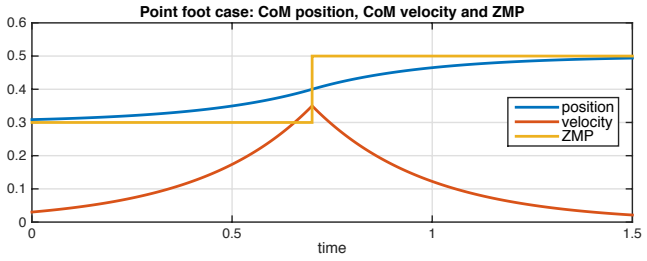

Fig. 4. Point foot case with instantaneous variation of the foot position

B. Simulation: constant single support

We now investigate and compare the results in the constant single support case; we have an optimal output transition problem between two constant values α^i_0 and α^f_0.

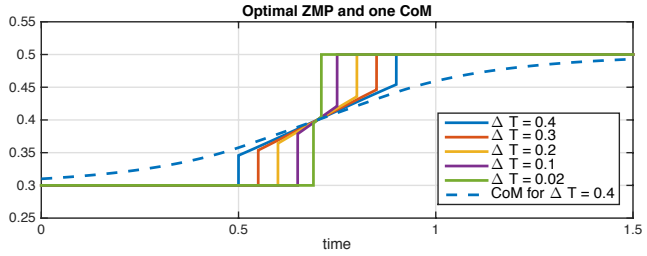

Fig. 5. Constant single support: resulting optimal ZMP as a function of the transition duration ΔT, also CoM position for $\Delta T = 0.4$s.

We note, from the optimal ZMP plots in Fig. 5 obtained for various values of the transition duration ΔT, that the optimal behavior requires a discontinuity in $x_{\rm zmp}$ at the transition times since during the single support we force the pendulum to have a constant ZMP. As soon as the ZMP is allowed to change, i.e. after t_i, it is moved forward but always slightly behind the CoM position (see the blue dashed line in Fig. 5

for an example) so that we continue falling forward but of the right amount. This shows how the optimal solution takes advantage of pre-actuation. Analogous considerations can be made for the discontinuity at t_f.

It is well-known that from an implementation point of view, discontinuities of the reference ZMP trajectory should be avoided [7]; however, the presented results are the outcome of a theoretical investigation, with respect to which any attempt to minimize energy should be compared.

Combining lateral and longitudinal motion, the ZMP, although being discontinuous, remains always in the support polygon of the double support phase thus guaranteeing a non-tilting motion.

Note that the transient acceleration is given by the control input (41) which, due to the e^{At} term with the specific cart-table A matrix, is linear w.r.t. t. Therefore the optimal CoM evolution during the transition will be cubic in time. We compare in Fig. 6 the CoM behavior w.r.t. the point foot case of (73) and Fig. 4, for various durations ΔT. As expected, while $\Delta T \to 0$, the CoM position tends to the limiting point foot case so that the deviation goes to 0.

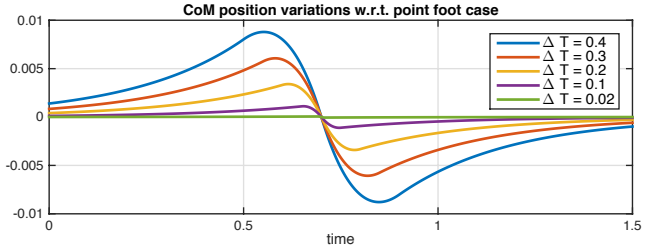

Fig. 6. Constant single support: reference CoM referred to (73) as a function of the transition duration ΔT

It is also quite intuitive, as displayed in Fig. 7, that as $\Delta T \to 0$ more effort is required since the CoM acceleration for the cart-table model (1) coincides with the control input.

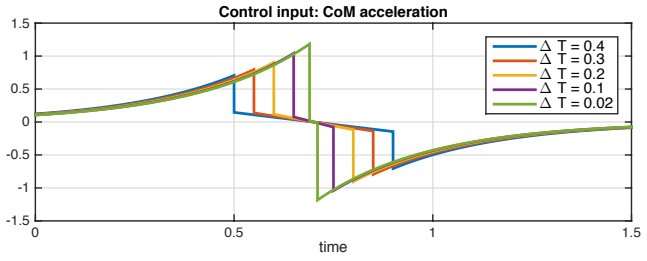

Fig. 7. Constant single support: control input as ΔT varies.

Finally we report an interesting comparison in Fig. 8 between the proposed Optimal Output Transition (OOT) solution and the usual approach of transforming an output transition into an optimal state transition one (OST) [9]. This alternative consists in letting the state evolve as x_c^* in the pre- and post- phases, and therefore no pre- and post-actuation is used, with a unique optimal state transfer during the transition phase.

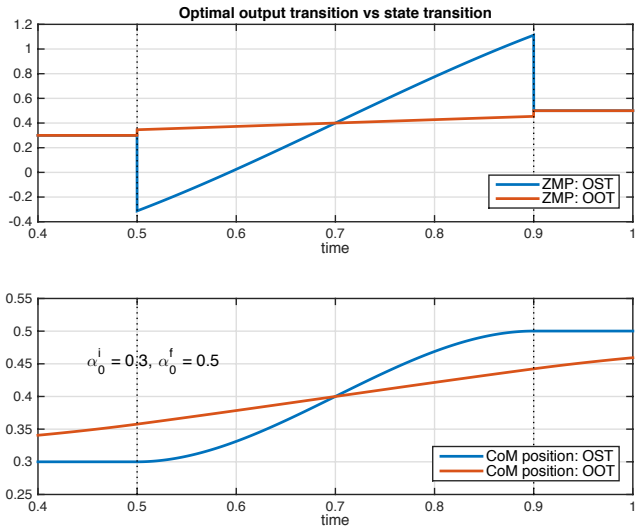

Fig. 8. Constant single support: with (OOT) or without (OST) pre/post actuation, ZMP and CoM position.

From the CoM plot, when no pre-actuation is done, at the switching time t_i the CoM is at $x_c^*(t_i) = 0.3$ and thus, for this constant case, it needs to get destabilized in order to move forward. This can be done only by making the ZMP go backwards, w.r.t. actual position, thus explaining the direction of the ZMP variation in t_i. While, when pre-actuation is allowed, the CoM starts moving forward before the end of the single support t_i even if the output (ZMP) is still constrained to remain constant, thus helping the following transition phase. The same applies for post-actuation.

C. Simulation: linear single support

In this set of simulations, we allow the ZMP to move linearly as in (62) with α_1^i and α_1^f both non-zero. This could model a heel-to-toe phase during single support thus providing a more natural motion as already suggested in [14] or [15]. The proposed analysis confirms, in an optimal energy perspective, this claim. In Fig. 9 we compare the optimal ZMP for various values of the slope coefficients α_1^i and α_1^f to the constant case ($\alpha_1^i = \alpha_1^f = 0$). The plots clearly show how the discontinuity can change as a function of the single support slope. In some situations it is also possible to find a particular linear profile for the single support ZMP which gives no ZMP discontinuity. A particular situation, helpful in lateral motion, is also reported when the two coefficients have different signs.

Finally the corresponding control inputs, after all we are considering a minimum energy problem, are shown in Fig. 10 where the better performance of linear single support is clearly evident. The case of the two slopes with different signs is a different case and should not enter in the comparison.

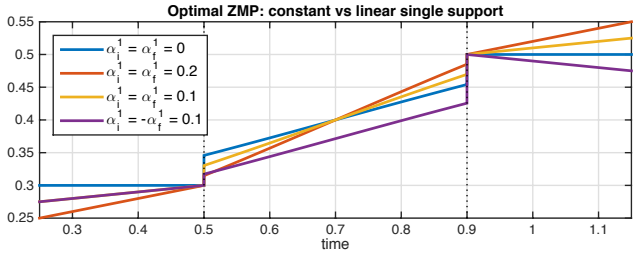

Fig. 9. Linear vs constant single support: ZMP.

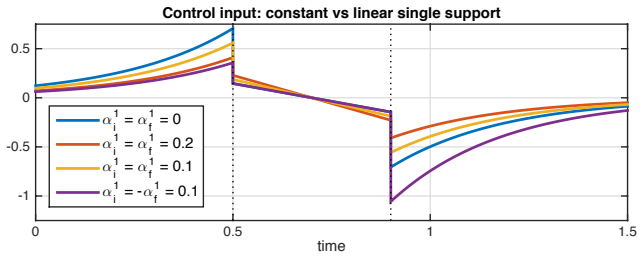

Fig. 10. Linear vs constant single support: control input.

IX. Conclusions

In this paper, we solved the problem of planning optimal zero moment point (ZMP) trajectories for the double support phase in bipedal gaits that alternate between single and double support. This was achieved by allowing pre- and post-actuation during the single support phases. As a byproduct, we provided a method to assess how the choice of desired ZMP trajectory during the single support phases impacts the overall energy expended during the footstep cycle.

In our future work, we plan to investigate the advantages of constraining the double support ZMP trajectory to belong to a generalized class of functions, to facilitate, for example, continuity in the ZMP trajectory. We also plan to study more general models of bipedal locomotion, including the three-mass model [22] which takes into account swing leg dynamics, and the flexible linear inverted pendulum, which includes elasticity [23]. We would also like to exploit the nice results of [24], for the exponential dichotomy of the inverted pendulum with variable height.

References

[1] S. Kajita, F. Kanehiro, K. Kaneko, K. Fujiwara, K. Harada, K. Yokoi, and H. Hirukawa, "Biped walking pattern generation by using preview control of zero-moment point," in *Proc. IEEE Int. Conference on Robotics and Automation (ICRA)*, vol. 2, 2003, pp. 1620–1626.

[2] K. Harada, S. Kajita, K. Kaneko, and H. Hirukawa, "An analytical method on real-time gait planning for a humanoid robot," in *Humanoid Robots (Humanoids), Proc. 4th IEEE/RAS International Conference on*, vol. 2, 2004, pp. 640–655.

[3] K. Harada, S. Kajita, F. Kanehiro, K. Fujiwara, K. Kaneko, K. Yokoi, and H. Hirukawa, "Real-time planning of humanoid robot's gait for force-controlled manipulation," *Mechatronics, IEEE/ASME Transactions on*, vol. 12, no. 1, pp. 53–62, Feb 2007.

[4] M. Morisawa, K. Harada, S. Kajita, K. Kaneko, F. Kanehiro, K. Fujiwara, S. Nakaoka, and H. Hirukawa, "A biped pattern generation allowing immediate modification of foot placement in real-time," in *Humanoid Robots (Humanoids), Proc. 6th IEEE-RAS International Conference on*, 2006, pp. 581–586.

[5] T. Buschmann, S. Lohmeier, M. Bachmayer, H. Ulbrich, and F. Pfeiffer, "A collocation method for real-time walking pattern generation," in *Humanoid Robots (Humanoids), Proc. 7th IEEE-RAS International Conference on*, 2007, pp. 1–6.

[6] K. Harada, K. Miura, M. Morisawa, K. Kaneko, S. Nakaoka, F. Kanehiro, T. Tsuji, and S. Kajita, "Toward human-like walking pattern generator," in *Intelligent Robots and Systems (IROS), IEEE/RSJ International Conference on*, 2009, pp. 1071–1077.

[7] T. Takenaka, T. Matsumoto, and T. Yoshiike, "Real time motion generation and control for biped robot -1st report: Walking gait pattern generation-," in *Intelligent Robots and Systems (IROS), Proc. IEEE/RSJ International Conference on*, 2009, pp. 1084–1091.

[8] S. Kajita, M. Morisawa, K. Miura, S. Nakaoka, K. Harada, K. Kaneko, F. Kanehiro, and K. Yokoi, "Biped walking stabilization based on linear inverted pendulum tracking," in *Intelligent Robots and Systems (IROS), Proc. IEEE/RSJ International Conference on*, 2010, pp. 4489–4496.

[9] H. Perez and S. Devasia, "Optimal output-transitions for linear systems," *Automatica*, vol. 39, no. 2, pp. 181 – 192, 2003.

[10] S. Kajita, H. Hirukawa, K. Harada, and K. Yokoi, *Introduction to Humanoid Robotics*. Springer Publishing Company, Inc., 2014.

[11] O. Urbann and S. Tasse, "Observer based biped walking control, a sensor fusion approach," *Autonomous Robots*, vol. 35, no. 1, pp. 37–49, 2013.

[12] L. Lanari, S. Hutchinson, and L. Marchionni, "Boundedness issues in planning of locomotion trajectories for biped robots," in *Humanoid Robots (Humanoids), Proc. 14th IEEE-RAS International Conference on*, 2014, pp. 951–958.

[13] L. Lanari and S. Hutchinson, "Planning desired center of mass and zero moment point trajectories for bipedal locomotion," in *Humanoid Robots (Humanoids), Proc. 15th IEEE-RAS 15th International Conference on*, 2015, pp. 637–642.

[14] K. Erbatur and O. Kurt, "Natural zmp trajectories for biped robot reference generation," *Industrial Electronics, IEEE Transactions on*, vol. 56, no. 3, pp. 835–845, 2009.

[15] S. Kajita, K. Miura, M. Morisawa, K. Kaneko, F. Kanehiro, and K. Yokoi, "Evaluation of a stabilizer for biped walk with toe support phase," in *Humanoid Robots (Humanoids), Proc. 12th IEEE-RAS International Conference on*, 2012, pp. 586–592.

[16] L. Lanari and S. Hutchinson, "Inversion-based gait generation for humanoid robots," in *Intelligent Robots and Systems (IROS), Proc. IEEE/RSJ International Conference on*, 2015, pp. 1592–1598.

[17] J. Englsberger, C. Ott, and A. Albu-Schaffer, "Three-dimensional bipedal walking control using divergent component of motion," in *Intelligent Robots and Systems (IROS), IEEE/RSJ International Conference on*, 2013, pp. 2600–2607.

[18] T. Koolen, T. de Boer, J. Rebula, A. Goswami, and J. Pratt, "Capturability-based analysis and control of legged locomotion, part 1: Theory and application to three simple gait models," *The International Journal of Robotics Research*, vol. 31, no. 9, pp. 1094–1113, 2012.

[19] A. Hof, M. Gazendam, and W. Sinke, "The condition for dynamic stability," *Journal of Biomechanics*, vol. 38, no. 1, pp. 1 – 8, 2005.

[20] T. Sugihara and Y. Nakamura, "Boundary condition relaxation method for stepwise pedipulation planning of biped robots," *Robotics, IEEE Transactions on*, vol. 25, no. 3, pp. 658–669, June 2009.

[21] K. Nishiwaki and S. Kagami, "Simultaneous planning of com and zmp based on the preview control method for online walking control," in *Humanoid Robots (Humanoids), Proc. 11th IEEE-RAS International Conference on*, Oct 2011, pp. 745–751.

[22] J. Park and K. Kim, "Biped robot walking using gravity-compensated inverted pendulum mode and computed torque control," in *Proc. IEEE Int. Conference on Robotics and Automation (ICRA)*, vol. 4, 1998, pp. 3528–3533.

[23] O. Urbann, I. Schwarz, and M. Hofmann, "Flexible linear inverted pendulum model for cost-effective biped robots," in *Humanoid Robots (Humanoids), Proc. 15th IEEE-RAS International Conference on*, 2015, pp. 128–131.

[24] J. Hauser, A. Saccon, and R. Frezza, "On the driven inverted pendulum," in *Proc. 44th IEEE Conference on Decision and Control*, 2005, pp. 6176–6180.